

# Enhanced PNF Probe Positioning in a Thermally-Uncontrolled Environment using Stable AUT Monuments

John H. Wynne, Farzin Motamed, George E. McAdams

NSI-MI Technologies, Torrance, CA, USA  
jwynne@nsi-mi.com, fmotamed@nsi-mi.com, gmcadams@nsi-mi.com

**Abstract**— The need for thermal stability in a test chamber is a well-established requirement to maintain the accuracy and repeatability sought for high frequency planar near-field (PNF) scanner measurements. When whole chamber thermal control is impractical or unreliable, there are few established methods for maintaining necessary precision over a wide temperature range.

Often the antenna under test (AUT) itself will require a closed-loop thermal control system for maintaining stable performance due to combined effects from transmission heat dissipation and the environment. In this paper, we propose a new approach for near-field system design that leverages this AUT stability, while relaxing the requirement of strict whole chamber thermal control. Fixed reference monuments strategically placed around the AUT aperture perimeter, when measured periodically with a sensing probe on the scanner, allow for the modeling and correction of the scanner positioning errors. This process takes advantage of the assumed stability of the reference monuments and attributes all apparent monument position changes to distortions in the scanner structure. When this monument measurement process is coupled with a scanner structure that can tolerate wide thermal variations, using expansion joints and kinematic connections, a robust structural error correction model can be generated using a bilinear mapping function. Application of such a structure correction technique can achieve probe positioning performance similar to scanners that require tightly controlled environments. Preliminary results as well as a discussion on potential design variations are presented.

**Keywords:** Near-Field, Accuracy, Alignment, Laser, Thermal Distortion, Precision Motion

## I. INTRODUCTION

Modern-day planar near-field scanners can achieve impressive global positioning accuracy, often to levels measured in microns [1]. To achieve this level of performance, designers are required to consider and control many factors. One of the most prominent is the control of temperature in the test chamber to within  $\pm 1$  °C, or better [1, 2]. Without this often-challenging restriction, constrained structural members can become significantly distorted due to unaccommodated thermal expansion or contraction. These structural distortions often

compound and introduce significant errors on the global positioning of the measurement probe.

### A. Two Methods for Moderate Chamber Thermal Drift Compensation

When strict temperature control is impractical or unreliable, a variety of methods have been used to account for thermal drift variation. In one method, a tracking laser is used to update a position error model for the probe [3]. This method, applied to a large horizontal PNF range, relies on a set of stable chamber retro-reflector monuments mounted to the floor and one at some elevation above the floor, which are measured by the tracking laser to update the range coordinate system. Concurrently, the scanner's moving bridge structure is characterized by measuring a set of retro-reflectors embedded within it. From these measurements, an error model is updated for real-time scan corrections. This method relies on a high level of operating coordination between the test measurement system, the tracking laser system and a live error model. The authors report successful operation over a temperature range of 2 °C.

In another method [1, 4] called motion tracking interferometry, the probe-to-AUT distance is estimated by near-field RF phase measurement at four spatially separated points during a planar scan. Over time, thermal effects will cause the measured offset values to drift. The measurement deltas are fit to a three degree-of-freedom (DOF) model of AUT solid-body motion (azimuth, elevation, and axial translation) then compensated by post-processing the near-field phase data. By measuring four points, the additional measured DOF affords the method the ability to determine measurement uncertainty by assuming no out-of-plane distortions are present. This method offers a simple solution for *relative* measurement errors attributed to thermal drift from several sources during a single scan, but there is no mention of an ability to address *absolute* measurement errors over time and multiple measurement scans. Within a single scan, however, the authors report [4] successful operation over a temperature range of 5 °C.

### B. A Method for In-Situ Testing of an Outdoor Radar System

Certain specialized antenna systems, such as ground-based and shipboard radar systems, increasingly require measurements

*in-situ*, where the test systems are permanently or temporarily co-located with the AUT. This class of measurement system poses additional challenges to the system designer, as the natural test volume may be influenced significantly by outdoor air temperature. The test system must be required to compensate not only for diurnal thermal variation, but also for seasonal thermal variation.

The method in [5] describes a portable vertical PNF system used to perform *in-situ* testing for the Aegis AN/SPY-1 shipboard radar array. During the setup sequence, the portable test-chamber, along with the 4.3 m x 4.3 m scanner, are assembled, transported and mounted to the side of a ship. The mounted test system, sealed to the side of the ship, provides the scanner with an environment that can be temperature-controlled by an environmental control unit (ECU). Once the test unit is in place, the ECU is powered, then the chamber and structure are allowed to reach a stable operating temperature. The temperature control system design includes ducting and pathways for controlled air around and through parts of the scanner structure in order to minimize transient structural distortions. Further, the system includes several laser systems for post-installed structural compensation: a straight-line laser interferometer to measure distance along X and Y, and a spinning laser system to measure deviations across the measurement Z plane. Once the system reaches stable operating temperature, these laser systems are used to perform a single characterization of the structural distortions for updating static error correction tables. No specific temperature range of operation is reported, though the ECU presumably allows for significant variation outside the enclosed test chamber.

### C. Leveraging the Stability of Radar Aperture Structures

The specific antenna systems addressed in the previous section, namely the ground-based and shipboard radar systems, for operational and reliability reasons, require that the thermal and structural stability of the antenna aperture is maintained to a high level, through cold plates connected to a liquid-cooled heat exchanger [6]. If we can assume the antenna aperture structure will maintain its stability even in an uncontrolled environment, this recognition allows for a novel design tradeoff: *relax the temperature control requirement in the test volume, leverage the assumed stability of the AUT, and allow the measurement system to adapt.*

While the methods reviewed previously have established merit for accommodating moderate to significant thermal change in the test environment, we propose consideration of a new method and system design with the following distinct advantages:

1. Tolerance to a wide temperature range in the test volume, with allowed variances of 30 °C, or greater;
2. Simple, robust and adaptive position error compensation system, using an onboard monument-sensing probe, adjacent to the microwave probe, positioned by the scanner to measure and estimate scanner distortions; and
3. Absolute position repeatability over long periods of time, across multiple measurement scans.

## II. OVERVIEW OF THE PROPOSED METHOD

### A. General Requirements and Assumptions

Before describing the proposed method, we should make explicit statements regarding the assumed state and external elements necessary for the successful application of this method.

1. The AUT aperture, or other suitably proximate structure, should be thermally controlled and structurally stable.
2. At least four monuments, representing the corners of the scan area, should be mounted to the AUT aperture surface, or other proximate stable structure.
3. The complete thermal cycle within the test volume should be relatively slow, such as might exist with a diurnal temperature cycle. Otherwise, more frequent measurement updates may be required.
4. The temperature distribution within the test volume should be moderately well mixed and should not contain any localized hot or cool spots which could alter the assumed structural behavior of the scanner.
5. There should be an independent method for detecting and controlling thermally induced phase changes in the RF measurement cable network.

### B. Error Correction Process

The basic implementation of the proposed method requires four physical monuments, mounted to and around the perimeter of the test article aperture, forming an approximate rectangle, as shown in Figure 1. During system calibration, the scanner moves to each monument and identifies the monument's location using a combination of scanner position, and data from a monument-sensing probe, mounted onboard the probe carriage, adjacent to the microwave probe. Based on the measured monument location, coordinate offsets for each monument are identified that normalize the monument set into a planar rectangle. Next, and separately, the scanner probe position errors are mapped using a tracking laser and applied to a static error correction table. These two pieces of data, the monument true locations in scanner space, and the probe position error map, would ideally be collected contemporaneously to form a snapshot of the scanner structural state at one time and temperature. This *golden* reference data set will be used during application of the error update process.

Once initiated, the error update process commands the scanner to move to each monument and sample its apparent location. Due to temperature change, or other structural disturbances, such as settling of the support structure or foundation, the monument location will appear to change from that measured during calibration. The net monument location differences are mapped to a 12 DOF bilinear model that transforms a planar rectangle to a non-planar quadrilateral. This transformation represents the change of the *golden* state of the monuments to the current, apparently distorted state. Since the baseline assumption is that the monument locations *do not* change, we conclude that the scanner has distorted, instead. To complete the process, the continuous bilinear mapping over the

entire probe space is inverted and superimposed onto the *golden* static error correction tables for use in the active dynamic probe correction scheme.

### C. Method Decomposition

The proposed method is logically divided into two complementary areas for discussion: the error measurement and correction system, and mechanical design features. As we will show, the simplicity of the error correction system requires inclusion of specific mechanical design features.

## III. ERROR MEASUREMENT AND CORRECTION SYSTEM

The general flow of the correction system is described in the method overview above. Further details about the physical monument targets, measurement devices, error modeling and application detail is provided in the sections below.

### A. Error Correction Table

The basis of the error correction system employed in this method is the static error correction table, used in on-the-fly dynamic probe positioning adjustments, including on-axis trigger mapping and cross-axis motion. This is a well-established technique to enhance probe positioning using 3-D coordinate data obtained from a tracking laser at system calibration [4, 7]. The method presented here updates the error correction table periodically, which is how probe positioning enhancements are realized.

### B. Monuments and Measurement Devices

In order to estimate the true location of a monument, it is important to discuss candidate physical representations of the monuments and sensing devices that can measure their locations. The device selection requirements should be consistent with the desired resolution necessary for the application. Together, the monuments and measurement devices form a target/sensor matched pair, and so should be defined and selected in reference to each other. Some tradeoffs to consider are: device cost, accuracy/repeatability, measurement speed, reliability, and integration complexity. Ultimately, the desired output should yield fast, repeatable 3-D coordinates of the monument feature.

For example, if a single-axis rangefinding laser is used as the measurement device, a well-defined hole may serve as the monument feature, along with a method to locate the center and surface of that hole. As another example, the measurement device may consist of a pair of high resolution cameras arranged for stereo-photogrammetry. In this instance, the monument may be well defined by a reticle located on the AUT surface.

The particular measurement device we used in our testing consisted of a line laser probe offered by Micro-Epsilon [8]. This type of device allowed for quick measurement and accurate coordinate identification of a physical monument body with a controlled circular profile.

### C. Error Model

Once monument locations are measured, an error model is used to predict scanner distortions at positions over the entire

scanner workspace. The error model chosen is a *bilinear mapping function* [9] which has the following characteristics:

- The mapping from the original domain to the distorted domain is fully described by 12 independent coefficients arranged in a 4x3 matrix, shown in (1), below. The model 12 DOFs matches the available measured monument 12 DOFs, and allows exact position convergence at each monument following update to the error correction table.
- The mapping fully models the following descriptive transformations/distortions in the scan plane: solid-body transformations (6 DOFs), uniform linear expansion or contraction of vertical or horizontal travel (2 DOFs), *trapezoidal keystoneing*, or linear differential shortening of vertical or horizontal travel across the scan plane (2 DOFs), *warping*, or non-planar torsion about vertical or horizontal axes (2 DOFs), and any combination of the above.
- Horizontal and vertical lines in the original domain remain linear in the distorted domain.
- Equispaced points along vertical and horizontal lines in the original domain remain equispaced in the distorted domain.

The bilinear mapping function takes the following vector form:

$$(x \ y \ z) = (uv \ u \ v \ 1) \begin{pmatrix} a & e & i \\ b & f & j \\ c & g & k \\ d & h & l \end{pmatrix} \quad (1)$$

where

$x, y, z$  distorted scanner positions

$u, v$  original scanner positions scaled to the *golden* monument locations whose rectangular corners are normalized to a unit square. Scanner positions within a patch boundary yield  $(u, v) \in \{0 : 1\}$

$a - l$  bilinear mapping parameters computed from the measured monument locations for each patch.

The basic error model utilizes a single set of four monuments, over which the entire scan plane distortions are derived. For larger scan planes, the scanner workspace may be divided into separate *patches*, or adjacent rectangular regions, each bounded by four monuments. An example of this is shown in Figure 4 and discussed further in Section VI. A separate bilinear mapping will be computed for each patch and will apply only to those scanner positions contained within the patch boundaries. Extrapolating the mapping outside a patch boundary, e.g.  $(u, v) \notin \{0 : 1\}$ , is continuous and defined, but may yield degraded performance when the extrapolation is large.

### D. Duration of the Monument Measurement Process

The measurement process duration is dictated by the scanner size, speed of axis motion, and the number of monuments to measure. For a moderately sized planner scanner (5 m x 5 m) using four monuments, the process will take typically less than five minutes to complete.

### E. Correction System Update Frequency

How often the process should run to update the static error correction table will depend on several factors, namely: thermal rise time in the operating test volume, duration of the update process relative to the total duration of antenna measurement scans, and allowable position repeatability tolerance. Recent experience has shown that an update period of two hours is a reasonable starting value.

## IV. MECHANICAL DESIGN FEATURES

### A. Overview

The error correction system presented above applies a bilinear mapping error model to measured changes in the monument locations. The assumed nature and success of this model depends on a graceful, linear reaction to temperature change by the scanner structure between the measured monuments. By measuring only discrete points around the perimeter, we have no knowledge of non-linear distortions between these points, so it is incumbent upon this method to require specific mechanical design features and considerations to impart such a thermally-benign behavior.

### B. Embodiment of Scanner and AUT

A vertical PNF scanner and AUT are shown in Figure 1. A scanner support structure, not shown, is assumed to fix the scanner rigidly to the AUT support structure. The scanner system is configured with a dual-drive X-axis, upper and lower, and a vertical bridge Y-axis driving the RF probe carriage. The probe carriage carries the monument sensing probe which is offset slightly from the RF open-ended waveguide (OEWG) probe. The AUT is shown in generic form, with four monuments located on its aperture perimeter. Several mechanical design features are highlighted, such as thermal expansion regions and additional rotational DOFs. These features will be discussed in further detail in the sections to follow.

### C. Beam Expansion Joints

When the test volume increases in temperature, a scanner beam element, such as the Y-axis bridge structure, for example, will increase in length by an amount proportional to its length. For example, a steel beam with a length of 10 m exposed to an increase in temperature of 10 °C will grow by 1.2 mm. Without an allowance for this expansion, the beam would likely distort, causing unwanted effects on positioning of the measurement probe. Further, if the temperature continues to rise, the constrained beam may cause failures at its anchor points and connection joints, affecting the basic functionality and life of the scanner system. Conversely, if the temperature decreases, the effect is similar: the beam will contract, impacting the system alignment and impairing basic functionality.

To counteract this effect, we have implemented basic expansion joints on all main structural beam elements, consisting of constrained rolling bearing elements that provide a low resistance path for thermal expansion or contraction in the axial direction. These degrees of freedom are labeled **EXP** in Figure 1. For the X-axis guideway beams anchored to the foundation, we fix one anchor position, and allowed the other to

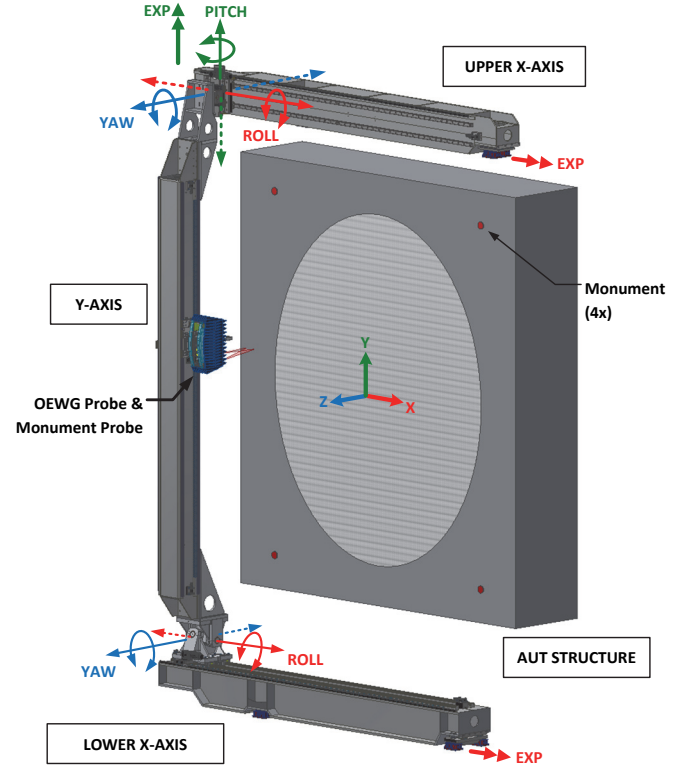


Figure 1. Vertical PNF scanner design with additional DOFs to account for thermal effects. AUT is shown with four perimeter monuments.

float in the axial direction. For the Y-axis bridge structure, we axially fix the bottom connection, and allow expansion at the upper connection.

Cross-axis expansion and contraction should be evaluated for the induced loads on constrained members, especially for beams anchored to concrete. Concrete and steel share a similar coefficient of thermal expansion [2], but foundational concrete will expand and contract at a different rate than exposed steel due to its greater *thermal inertia*, or resistance of a body's change in temperature relative to its surroundings. If necessary, slip-joints made from low friction materials, such as PTFE or oil-impregnated bronze, can be employed which allow small motions to relieve induced stresses when cross-axis loads exceed designed thresholds.

### D. Reduced Moment Coupling Connections

When moment connections are employed between moving structural elements, there exists an opportunity for transmitted distortion. This is especially true for the example in Figure 1. If the lower X-axis and upper X-axis guideways become misaligned due to thermal changes in the support structure, or foundational drift, the Y-axis bridge structure, spanning both guideways, will be subject to induced loads and distortion, if moment connections are used.

To counteract this, our model scanner was designed with additional rotational DOFs to both the lower and upper X-axis-

to-bridge connections, designated as **YAW**, **PITCH**, and **ROLL** in Figure 1. Implemented as cardan gimbals, these jointed connections allow the bridge structure to avoid receiving distortion-inducing moments from guideway misalignments. Note that, for stability, the lower X-axis requires a moment connection about the Y-axis, so does not contain a DOF in the **PITCH** direction.

### E. Miscellaneous Design Considerations

Other selection criteria should be considered in the design of structures and joints, as follows.

1) *Material Selection*: Choosing dissimilar materials, especially at critical joint boundaries, may induce thermal strains sufficient to cause unwanted misalignments. This may be especially true for components located near the probe assembly, where lightweight aluminum parts are mated with structural steel members. Our scanner implementation primarily includes steel components and structures. But where components required aluminum material selection, such as the probe polarization rotator, and cable management structure, allowances for differential expansion of steel and aluminum parts were implemented using slots and flexures.

2) *Symmetric Beam Cross-Sections*: Even when uniform temperature change is assumed across a beam element, uneven heat transfer and localized thermal inertia may cause unwanted out-of-plane beam distortion and curvature. In our implementation, considerable effort was made to ensure symmetric beam elements were utilized where possible. In this way, expansion of localized mass units is balanced by expansion of similar mass units diametrically opposed on the structural member's neutral axis.

3) *Section Thickness*: We have introduced the idea of thermal inertia in concrete which suggests that a heavier object with the same exposed area will react more slowly to induced thermal changes. So it follows as well that thicker structural steel sections will react more slowly to induced thermal change than thinner steel sections, with the same exposed surface area. Unfortunately, utilizing heavy steel sections universally, while decreasing short term transient thermal effects, has the practical disadvantage in that moving heavier structural members requires larger, more powerful motors and capable drivetrains. Also, structural resonance frequencies are lowered by increased structural mass, which can be detrimental to scanner performance. The approach we considered in our design was to make static structural members as heavy as possible within reasonable bounds, and to match the wall thicknesses of elements in close proximity. For example, a carriage plate mounted to linear bearings should match the wall thickness of the underlying structural member beneath the linear bearing rails.

## V. PRELIMINARY RESULTS

A vertical PNF scanner covering a scan area of 42 m<sup>2</sup> was recently delivered. Over the course of nine days, the interior test volume temperature varied by 21 °C. The error measurement and correction system, as well as the mechanical design features were implemented on this system, including four perimeter monuments attached to the AUT.

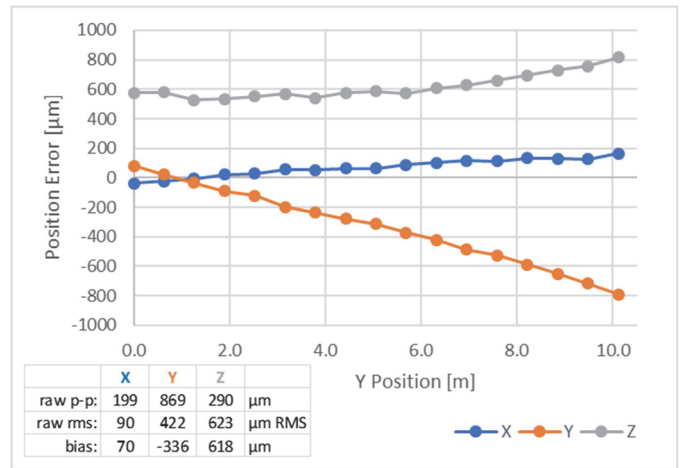


Figure 2. Sampled XYZ probe position errors *before* monument update corrections.

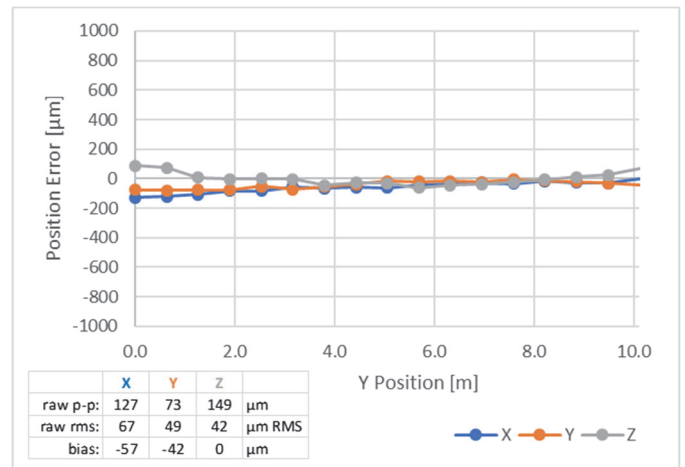


Figure 3. Sampled XYZ probe position errors *after* monument update corrections.

A tracking laser was used to perform calibration of the scanner probe positioning errors at an initial time and temperature. Then after several days, and a temperature change of 11 °C from calibration, the laser was used to evaluate the absolute probe position repeatability, corrected using the system and methods described in this paper.

The results in Figure 2 show that the maximum un-enhanced XYZ position errors are **623 µm RMS** before monument update corrections were applied. As shown in Figure 3, the maximum enhanced XYZ position errors are reduced to **67 µm RMS** after monument update corrections were applied.

While the test system described was only evaluated for a maximum chamber temperature variation of 11 °C, results are promising and on par with many systems having stable thermal conditions [4].

## VI. MONUMENT SET VARIATIONS

### A. Multi-patch Monument Sets

When the scanner workspace becomes large, the X-axis guideways may require multiple mounting anchors to properly support the bridge payload. In this case, monuments should be aligned with the X-axis mounting anchors, as any beam non-linearities, emergent from thermal or structural variances, will be likely to originate here.

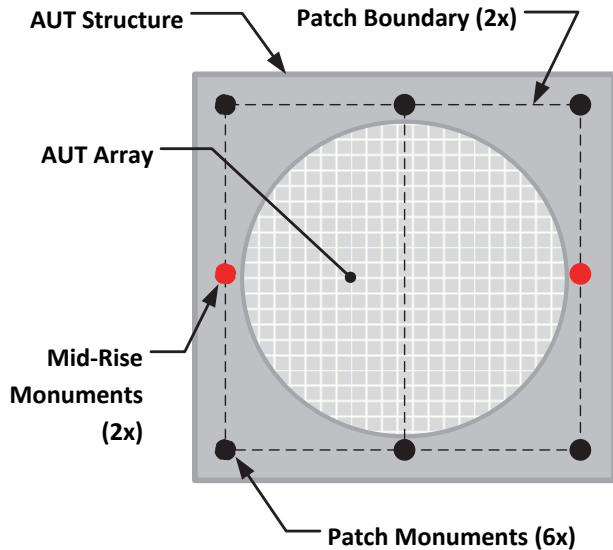


Figure 4. An eight-monument set mounted to the AUT structure, configured into two patches with two mid-rise monuments.

Having additional monuments allows us to introduce the concept of a multi-patch environment, shown with two patches in Figure 4. Multiple patches require separate bilinear mappings for each patch. Then, the scan plane error mapping requires selection of the appropriate patch and bilinear mapping from which to apply the distortion update. Of course, measuring additional monuments will increase the update process duration, a disadvantage, and should be weighed carefully with other desired objectives.

### B. Mid-rise Monuments

Our recent observations indicate that for the vertical scanner model shown in Figure 1, when the bridge structure is lengthened to accommodate longer vertical travel, the bridge

structure may become increasingly sensitive to biased heating, from sources such as solar radiation or night sky cooling, exhibiting unwanted curvature. To counteract this, we propose an enhancement to the monument model which includes an additional monument halfway up each side of the patch, as shown in Figure 4. Evaluating this monument location change would allow for an independent curvature model, in X and Z directions, that can be superimposed onto the combined static error and bilinear mapping error correction table.

## VII. CONCLUSIONS

The method proposed in this paper describes a new approach to near-field system design when test volume temperature cannot be assured or is impractical. The approach leverages the structural stability of particular antenna systems under test and matches a simple error correction model with thoughtful mechanical design features that accommodate large temperature variation while minimizing induced structural distortions. Preliminary results show that the method performs as intended over a temperature range at least an order of magnitude greater than typical near-field test environments. Finally, with additional modifications to model first order curvature effects on the moving structure, further reductions in residual errors may be realized.

## REFERENCES

- [1] D. Slater, "A 550 GHz near-field antenna measurement system for the NASA sub-millimeter wave astronomy satellite," AMTA Proceedings, October 1994.
- [2] T. Schwartz, E. Kim, "Precision motion in highly accurate mechanical positioning," AMTA Proceedings, November 2012.
- [3] S. T. McBride, S. R. Nichols, "Closed-loop real-time PNF position compensation with a tracking laser," AMTA Proceedings, November 2014.
- [4] G. Hindman, "Design and implementation of large planar near-field measurement systems for satellite antenna measurements," Presentation from [https://www.nsi-mi.com/images/Technical\\_Papers/Articles/Design-and-Implementation-of-Large-Planar-Near-field-Measurement-Systems-for-Satellite-Antenna-Measurements.pdf](https://www.nsi-mi.com/images/Technical_Papers/Articles/Design-and-Implementation-of-Large-Planar-Near-field-Measurement-Systems-for-Satellite-Antenna-Measurements.pdf), March 2011.
- [5] G. E. McAdams, R. Romanchuk, "14' x 14' portable planar near-field scanner system (PPNFSS) for the Aegis array," AMTA Proceedings, November 1999.
- [6] A. K. Agrawal, B. A. Kopp, M. H. Luesse, K. W. O'Haver, "Active phased array antenna development for modern shipboard radar systems," Johns Hopkins APL Technical Digest, p. 600-613, Vol 22, Num 4, 2001.
- [7] G. Hindman, "Position correction on large near-field scanners using an optical tracking system," AMTA Proceedings, October 1994.
- [8] Micro-Epsilon product catalog, "scanCONTROL compact laser profile sensors", 2018.
- [9] P. S. Heckbert, "Fundamentals of Texture Mapping and Image Warping," Master's Thesis, University of California, Berkeley, 1989.